Comparative Analysis of Colon Cancer-Derived *Fusobacterium nucleatum* Subspecies: Inflammation and Colon Tumorigenesis in Murine Models

Jessica Queen,[a] Jada C. Domingue,[a] James Robert White,[b] Courtney Stevens,[a] Barath Udayasuryan,[c] Tam T. D. Nguyen,[d] Shaoguang Wu,[a] Hua Ding,[e] Hongni Fan,[f] Madison McMann,[a] Alina Corona,[a] Tatianna C. Larman,[g] Scott S. Verbridge,[c] Franck Housseau,[f,h] (ID) Daniel J. Slade,[d] Julia L. Drewes,[a] (ID) Cynthia L. Sears[a,e,f,h]

aDepartment of Medicine, Johns Hopkins University, Baltimore, Maryland, USA
bResphera Biosciences, Baltimore, Maryland, USA
cDepartment of Biomedical Engineering and Mechanics, Virginia Polytechnic Institute, Blacksburg, Virginia, USA
dDepartment of Biochemistry, Virginia Polytechnic Institute, Blacksburg, Virginia, USA
eDepartment of Molecular Microbiology and Immunology, Johns Hopkins Bloomberg School of Public Health, Baltimore, Maryland, USA
fDepartment of Oncology, Johns Hopkins University, Baltimore, Maryland, USA
gDivision of Gastrointestinal and Liver Pathology, Johns Hopkins University, Baltimore, Maryland, USA
hBloomberg-Kimmel Institute, Johns Hopkins University, Baltimore, Maryland, USA

Jessica Queen and Jada C. Domingue contributed equally to this work. Author order was determined by who completed the final experiments for the manuscript.

ABSTRACT Fusobacteria are commonly associated with human colorectal cancer (CRC), but investigations are hampered by the absence of a stably colonized murine model. Further, *Fusobacterium nucleatum* subspecies isolated from human CRC have not been investigated. While *F. nucleatum* subspecies are commonly associated with CRC, their ability to induce tumorigenesis and contributions to human CRC pathogenesis are uncertain. We sought to establish a stably colonized murine model and to understand the inflammatory potential and virulence genes of human CRC *F. nucleatum*, representing the 4 subspecies, *animalis*, *nucleatum*, *polymorphum*, and *vincentii*. Five human CRC-derived and two non-CRC derived *F. nucleatum* strains were tested for colonization, tumorigenesis, and cytokine induction in specific-pathogen-free (SPF) and/or germfree (GF) wild-type and *Apc*^*Min/+* mice, as well as *in vitro* assays and whole-genome sequencing (WGS). SPF wild-type and *Apc*^*Min/+* mice did not achieve stable colonization with *F. nucleatum*, whereas certain subspecies stably colonized some GF mice but without inducing colon tumorigenesis. *F. nucleatum* subspecies did not form *in vivo* biofilms or associate with the mucosa in mice. *In vivo* inflammation was inconsistent across subspecies, whereas *F. nucleatum* induced greater cytokine responses in a human colorectal cell line, HCT116. While *F. nucleatum* subspecies displayed genomic variability, no distinct virulence genes associated with human CRC strains were identified that could reliably distinguish these strains from non-CRC clinical isolates. We hypothesize that the lack of *F. nucleatum*-induced tumorigenesis in our model reflects differences in human and murine biology and/or a synergistic role for *F. nucleatum* in concert with other bacteria to promote carcinogenesis.

IMPORTANCE Colon cancer is a leading cause of cancer morbidity and mortality, and it is hypothesized that dysbiosis in the gut microbiota contributes to colon tumorigenesis. *Fusobacterium nucleatum*, a member of the oropharyngeal microbiome, is enriched in a subset of human colon tumors. However, it is unclear whether this genetically varied species directly promotes tumor formation, modulates mucosal immune responses, or merely colonizes the tumor microenvironment. Mechanistic studies to address these questions have been stymied by the lack of an animal model that does not rely on daily orogastric gavage. Using multiple murine models, *in vitro* assays with a human

colon cancer cell line, and whole-genome sequencing analysis, we investigated the proinflammatory and tumorigenic potential of several *F. nucleatum* clinical isolates. The significance of this research is development of a stable colonization model of *F. nucleatum* that does not require daily oral gavages in which we demonstrate that a diverse library of clinical isolates do not promote tumorigenesis.

KEYWORDS *Fusobacterium* subspecies, colorectal cancer, mouse models, *Fusobacterium* genome sequences, *Fusobacterium* virulence, *Fusobacterium*

*F*usobacterium nucleatum is a Gram-negative anaerobe common to the human oral cavity of healthy individuals and those with periodontal disease (1). A heterogenous species consisting of four subspecies, *animalis*, *nucleatum*, *polymorphum*, and *vincentii*, *F. nucleatum* is the most abundant bacterium in dental plaque biofilms, where it functions as a bridging species to facilitate aggregation and invasion of other bacteria (2–6). *F. nucleatum* is also the oral organism most commonly associated with nonoropharyngeal diseases, including inflammatory bowel disease, atherosclerosis, organ abscesses, adverse pregnancy outcomes, and, more recently, colorectal cancer (CRC) (1, 7, 8). Clinical studies of North American, European, and Asian cohorts have established that *F. nucleatum* is enriched in a subset of CRC compared to both paired normal colonic tissues and healthy controls (7–11). What remains unknown is whether *F. nucleatum* initiates tumor development, promotes tumor progression, or is simply an opportunistic colonizer of the tumor microenvironment.

The association of *F. nucleatum* with the tumor microenvironment of CRC was first established by several groups using sequencing technologies (7, 8, 12). For instance, Castellarin et al. used RNA sequencing analysis of CRC patients to reveal the overabundance of *Fusobacterium* sequences in tumor tissues compared to matched normal tissues (7). Additionally, two subsequent papers suggested *F. nucleatum*'s ability to promote and potentiate intestinal tumorigenesis in murine models (13, 14). In one study, daily orogastric inoculation of a Crohn's disease-derived *F. nucleatum* isolate (EAVG_002; 7/1) into multiple intestinal neoplasia ($Apc^{Min/+}$) mice resulted in modest (median, one colon tumor per $Apc^{Min/+}$ mouse) induction of colonic tumorigenesis compared to sham or *Streptococcus* species controls (median, no colon tumors per $Apc^{Min/+}$ mouse), with tumorigenesis linked to induction of myeloid cell inflammation (13). Further evidence for the role of *F. nucleatum* in tumorigenesis was demonstrated using an HCT116 cell murine xenograft model (14). Mice injected with purified FadA, one of *F. nucleatum*'s adhesion factors, showed a 20% increase in xenograft growth compared to mutant FadA protein or bovine serum albumin (BSA) controls, suggesting that FadA contributes to *F. nucleatum*-associated tumorigenesis.

Additional murine models, as well as *in vitro* investigations with CRC-derived cell lines, have sought to better understand any potential causal role that *F. nucleatum* plays in CRC (15–21). Studies led by Abed et al. (15, 21) established Fap2 as a lectin, binding to host Gal-GalNAc to mediate *F. nucleatum* association with colon tumors and CRC cell lines; Fap2 mutants showed reduced binding. Importantly, *F. nucleatum* localized to tumors via intravenous (i.v.) injection using the CT26 orthotopic mouse model (15). This was supported by a follow-up study directly comparing i.v. injection to oral gavage of *F. nucleatum* in which intravenously administered *F. nucleatum* was more successful in tumor colonization (21). Mechanistic insights have implicated Toll-like receptor 4 (TLR4)-β-catenin and TLR4-MYD88 pathways underlying *F. nucleatum* action in CRC and *F. nucleatum* induction of microRNAs activating autophagy to promote chemoresistance (16, 19, 20). A few studies support antibacterial therapies for alleviation of *F. nucleatum*-associated CRC. Berberine, an isoquinoline alkaloid used to treat intestinal infections in China, reduced colon tumor numbers in mice inoculated daily with *F. nucleatum* compared to those with *F. nucleatum* alone (18). Additionally, metronidazole treatment of a CRC patient-derived xenograft model reduced tumor growth, proliferation, and *F. nucleatum* tumor load (17).

TABLE 1 *F. nucleatum* strains used in this study

Strain name	Abbreviated designation	Subspecies	Source (reference)
F. nucleatum 173CP[a]	CRC-*F. nucleatum* subsp. *animalis*	*animalis*	CRC patient, Spanish cohort
CTX3 *F. nucleatum* 10[a]	CRC-*F. nucleatum* subsp. *nucleatum*	*nucleatum*	CRC patient, Spanish cohort
F. nucleatum 146CP[a]	CRC-*F. nucleatum* subsp. *vincentii*	*vincentii*	CRC patient, Spanish cohort
F. nucleatum 3760T	Clumpy CRC-*F. nucleatum* subsp. *polymorphum*	*polymorphum*	CRC patient, US cohort
F. nucleatum S043-1	Nonclumpy CRC-*F. nucleatum* subsp. *polymorphum*	*polymorphum*	CRC patient from Malaysian cohort
F. nucleatum EAVG_002[c]	Non-CRC-*F. nucleatum* subsp. *animalis*	*animalis*	IBD[b] patient (63)
F. nucleatum 23726	Non-CRC-*F. nucleatum* subsp. *nucleatum*	*nucleatum*	Urogenital tract (ATCC)

[a]Strain provided by S. Bullman, Fred Hutchinson Cancer Research Center, Seattle, WA.
[b]IBD, irritable bowel disease.
[c]*F. nucleatum* EAVG_002 is also known as *F. nucleatum* 7/1.

However, no studies have developed a murine model of stable colonic *F. nucleatum* colonization, nor have there been comparative analyses of the tumorigenic potential of the *F. nucleatum* subspecies in existing CRC murine models. To date, which *F. nucleatum* subspecies may be most relevant to human CRC pathogenesis remains uncertain, although limited data suggest *F. nucleatum* subspecies *animalis* is more frequently present in CRC tissues (22). Importantly, studies evaluating the effect of long-term daily orogastric gavage with *F. nucleatum* do not reflect the expected events in human disease in which either passage through the gastrointestinal tract or transient bacteremia facilitates stable colonization of the colon and/or colon tumors. Thus, we tested approaches to develop a murine model of stable intestinal colonization, in contrast to daily oral gavages, while also investigating the inflammatory and tumorigenic potential of several genetically diverse CRC- and non-CRC-derived *F. nucleatum* subspecies in both mice and the CRC cell line HCT116.

RESULTS

CRC-derived *F. nucleatum* subspecies do not consistently colonize SPF mice. While several studies have investigated the role that *F. nucleatum* plays in gut inflammation and tumorigenesis, those studies failed to report stable colonization of *F. nucleatum*, and the reported pathophysiological changes were dependent on daily *F. nucleatum* gavages (13, 16, 18, 23, 24). Additionally, these studies did not investigate CRC-derived *F. nucleatum* strains. Herein, we used *F. nucleatum* strains isolated from human CRC tumor biopsy specimens, representing each of the subspecies and from diverse geographic locations (Table 1), and assessed whether CRC-derived *F. nucleatum* colonized the mouse gut, using antibiotic-treated specific-pathogen-free (SPF) C57BL/6J wild-type (WT) mice inoculated weekly with CRC-derived *F. nucleatum* strains. Despite repeated orogastric inoculations, all *F. nucleatum* isolates failed to establish consistent colonic colonization (Fig. 1A). Only mice gavaged with the CRC-derived *F. nucleatum* subsp. *vincentii* (CRC-*F. nucleatum* subsp. *vincentii*) reached levels above the limit of detection (LOD), but only following the fourth and final gavage; this signal was quickly lost by 12 days after the final inoculation. Further, mice gavaged with CRC-*F. nucleatum* subsp. *vincentii* failed to exhibit weight loss or changes in colon length typically seen with inflammation/colitis (25) (data not shown). Because data suggest that host-gene microbe interactions affect pathogenesis (26), we further tested CRC-*F. nucleatum* subsp. *vincentii* in SPF *Apc*^Min/+^ mice. Despite an intensified orogastric gavage protocol (see Materials and Methods), CRC-*F. nucleatum* subsp. *vincentii* was unable to colonize the mice (Fig. S1 in the supplemental material). Thus, we conclude that CRC-derived *F. nucleatum* subspecies do not stably colonize the gut of conventionally raised SPF mice, even with repeated inoculations that are typically not necessary with other enteric pathogens.

CRC-derived *F. nucleatum* subsp. differentially colonize GF mice. Due to the lack of stable colonization in SPF mice, we hypothesized that, despite the use of microbiome-disrupting antibiotic treatment, *F. nucleatum* remained unable to overcome competition by the modified microbiota. Thus, we turned to a germfree (GF) murine model. GF wild-type (WT) mice were inoculated once with CRC-derived *F. nucleatum* isolates, and colonization was assessed after 14 days. We found that *F. nucleatum*
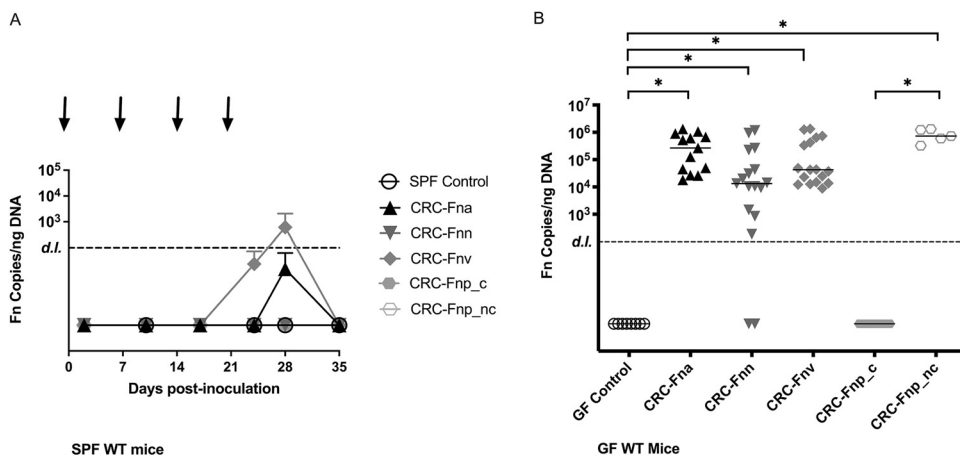
FIG 1 Differential colonization of *F. nucleatum* subspecies in SPF and GF wild-type (WT) mice. (A) SPF mice were orally gavaged with the designated *F. nucleatum* subspecies at days 0, 7, 14, and 21 (arrows), and fecal pellets were collected at the indicated time points on the *x* axis. *F. nucleatum* colonization is plotted as *F. nucleatum* copies/ng fecal DNA per group over time (mean ± SD), with a detection limit (LOD) of 100 *F. nucleatum* copies. *n* = 3 control mice and 10 experimental mice per strain. (B) GF WT mice were orally gavaged with *F. nucleatum* once and then assessed for colonization after 14 days. Each dot indicates the *F. nucleatum* copies/ng DNA of an individual mouse. Bars indicate the median with interquartile range. (*Fna* denotes *F. nucleatum* subsp. *animalis*, *Fnn* denotes *F. nucleatum* subsp. *nucleatum*, *Fnv* denotes *F. nucleatum* subsp. *vincentii*, *Fnp_c* denotes clumpy *F. nucleatum* subsp. *polymorphum*, and *Fnp_nc* denotes nonclumpy *F. nucleatum* subsp. *polymorphum*). *n* = 5 to 17 mice/group. One GF control mouse calculated as having 125 *F. nucleatum* copies/ng DNA was removed from analysis.

subsp. differed in their ability to colonize GF WT mice (Fig. 1B). In contrast to the SPF model, CRC-derived *F. nucleatum* subsp. *animalis* (CRC-*F. nucleatum* subsp. *animalis*), CRC-*F. nucleatum* subsp. *nucleatum*, and CRC-*F. nucleatum* subsp. *vincentii* displayed significant colonization levels compared to GF controls ($P < 0.0001$, $P = 0.001$, and $P < 0.0001$, respectively). Notably, a minority of mice (3/17) inoculated with *F. nucleatum* subsp. *nucleatum* failed to colonize, although those that did were colonized at levels similar to *F. nucleatum* subsp. *animalis* and *F. nucleatum* subsp. *vincentii*. Interestingly, the CRC-derived *F. nucleatum* subsp. *polymorphum* initially tested was unable to colonize the mice. We hypothesized that this may be due to its clumpy, self-aggregative morphology when grown *in vitro* (Fig. S2). We therefore inoculated a group of mice (*n* = 5) with a nonclumpy CRC-derived *F. nucleatum* subsp. *polymorphum* strain (nonclumpy CRC-*F. nucleatum* subsp. *polymorphum*), which significantly colonized the mice compared to the clumpy strain ($P = 0.0005$) and GF controls ($P = 0.0008$) and to levels similar to the other isolates; however, it was also unable to colonize SPF WT mice (Fig. 1A).

As *F. nucleatum* contributes to biofilm development of oral dental plaques and is also present in a majority of CRC-associated colonic biofilms (27), we also assessed distal colons for the presence of *F. nucleatum* biofilms by fluorescent *in situ* hybridization (FISH). Despite stable colonization of most *F. nucleatum* subsp. in GF WT mice, mucus-invasive biofilms were not found. Only 3/21 mice (14%) evaluated displayed mucosal staining with the all-bacterial or *Fusobacterium*-specific probe (Fig. S3). Thus, while prior data support that *F. nucleatum* stably colonizes the gut of monognotobiotic mice (28), our colonization data suggest variable colonization potential of *F. nucleatum* isolates with very limited mucosal association in gnotobiotic mice.

CRC-derived *F. nucleatum* subspecies do not differ in induction of proinflammatory gene expression in GF WT mice. Having demonstrated that GF mice allow for significant colonization of several CRC-derived *F. nucleatum* strains, we next investigated whether *F. nucleatum* colonization impacts inflammatory gene expression in the distal colon. Despite robust colonization by *F. nucleatum* subsp. *animalis*, *F. nucleatum* subsp. *vincentii*, *F. nucleatum* subsp. *nucleatum*, and nonclumpy *F. nucleatum* subsp. *polymorphum* (Fig. 1B), we found no significant changes in expression of several cytokine and
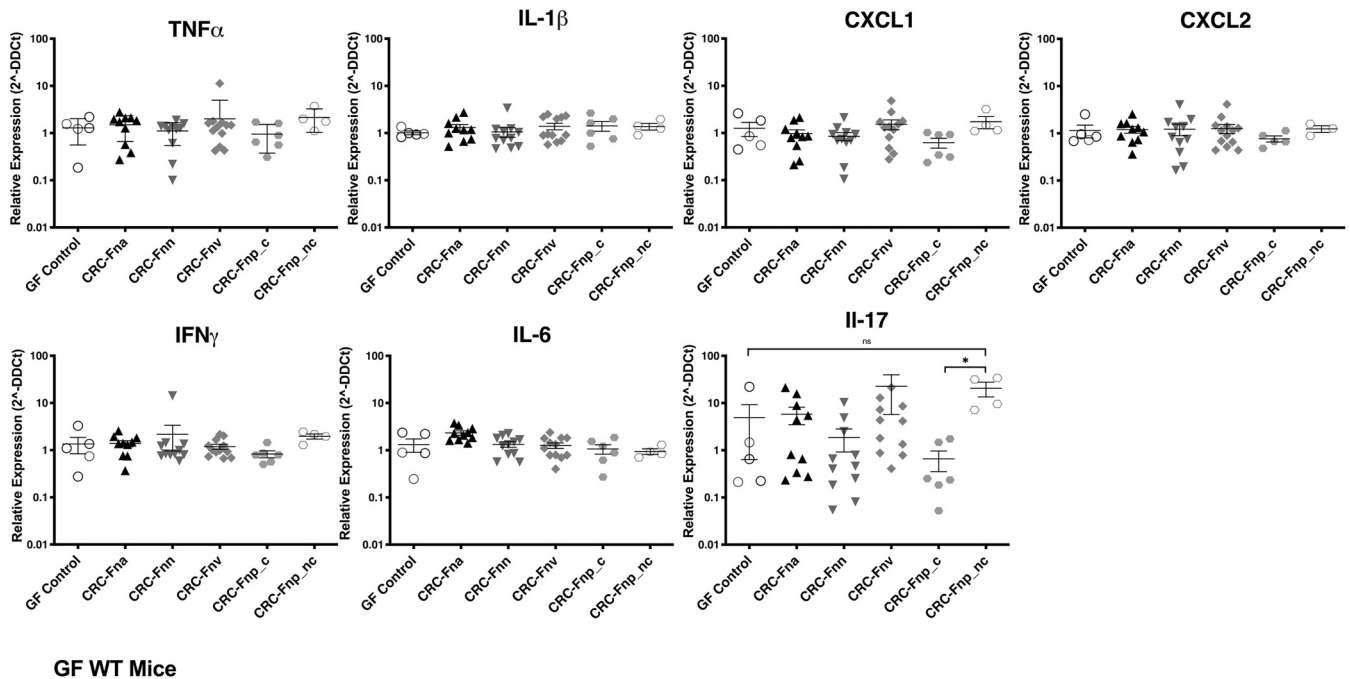
FIG 2 Changes in distal colon inflammatory gene expression. GF WT mice were inoculated with the indicated *F. nucleatum* strains then harvested after 14 days. RNA was extracted from distal colon tissue, and relative quantification of gene expression was performed with qRT-PCR using TaqMan gene expression Assays for each target gene, normalized to murine GAPDH. Data are plotted as the relative expression (threshold cycle [$2^{-\Delta\Delta CT}$]) per mouse. Bars indicate the median with interquartile range. n = 5 to 17 mice/group. (*Fna* denotes *F. nucleatum* subsp. *animalis*, *Fnn* denotes *F. nucleatum* subsp. *nucleatum*, *Fnv* denotes *F. nucleatum* subsp. *vincentii*, *Fnp_c* denotes clumpy *F. nucleatum* subsp. *polymorphum*, and *Fnp_nc* denotes nonclumpy *F. nucleatum* subsp. *polymorphum*).

chemokine genes in the distal colon compared to GF control mice (Fig. 2). While the majority of genes had very similar expression across groups compared to the GF controls, expression of interleukin 17a (IL-17a) was highly variable within and across groups. Notably, the nonclumpy *F. nucleatum* subsp. *polymorphum* strain significantly upregulated IL-17a expression in comparison to the clumpy *F. nucleatum* subsp. *polymorphum* isolate (P = 0.0095); however, this still did not differ from the GF controls (P = 0.0635). Further, IL-17 levels did not correlate with *F. nucleatum* copy number (linear regression; P = 0.11, R^2 = 0.06). Similar to SPF mice, there were no changes in body weight or colon length in GF WT mice (data not shown).

F. nucleatum subsp. differ in colonization and induction of proinflammatory gene expression but do not promote tumorigenesis in GF _Apc^Min/+_ mice. Since previous studies in murine models showed a strong link between inflammation and colon tumorigenesis (29), we expected that, over time, *F. nucleatum* would alter the immune microenvironment of mice susceptible to intestinal tumorigenesis and promote colon tumors. For these experiments, GF *Apc*$^{Min/+}$ mice were gavaged weekly for 4 weeks. Similar to our findings in GF WT mice (Fig. 1B), we observed differences in colonization of GF *Apc*$^{Min/+}$ mice (Fig. 3A), with delayed uptake of the clumpy *F. nucleatum* subsp. *polymorphum* strain and lack of persistent colonization in mice inoculated with the CRC-*F. nucleatum* subsp. *nucleatum* strain. Numerous mice gavaged with each subspecies were able to clear *F. nucleatum* after weekly inoculations ceased; only 47% (24/51 mice) remained colonized at the end of the 11-week experiments. In contrast to previous studies with daily inoculation of *F. nucleatum* in SPF *Apc*$^{Min\Delta850/+}$ mice (13), but similar to studies in gnotobiotic *Apc*$^{Min\Delta850/+}$ mice inoculated weekly with *F. nucleatum* (28), we found that stable colonization of GF *Apc*$^{Min/+}$ mice with CRC-derived *F. nucleatum* strains was not associated with an increase in colon tumors (Fig. 3B). Overall, 1 tumor was detected in 17 of 57 (30%) of GF *Apc*$^{Min/+}$ mice gavaged with *F. nucleatum* subsp., and only 1 mouse displayed 2 tumors. Further, when we tested two non-CRC-derived *F. nucleatum* subsp. *animalis* and *F. nucleatum* subsp. *nucleatum* strains
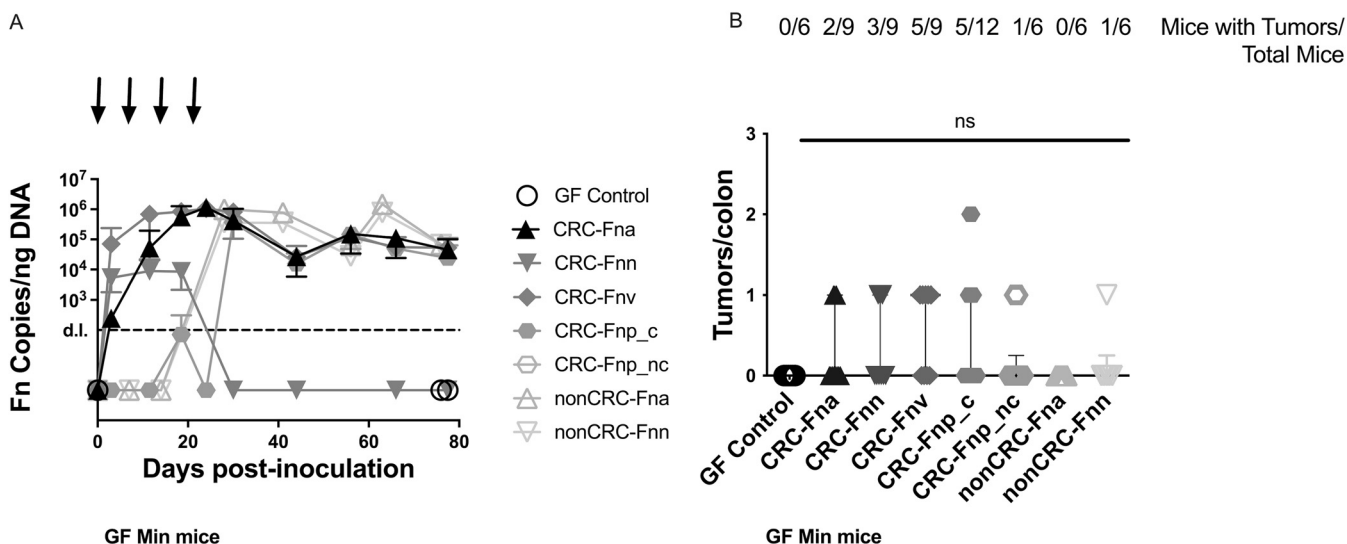
FIG 3 Colonization and tumorigenesis in *F. nucleatum*-treated GF *Apc*[Min/+] mice. GF *Apc*[Min/+] mice were orally gavaged once per week for 4 weeks (arrows), and fecal pellets were collected at the indicated time points on the *x* axis. (A) Colonization is plotted as *F. nucleatum* copies/ng fecal DNA per group over time (mean ± SD) with a detection limit (LOD) of 100 *F. nucleatum* copies. (B) Data are displayed as number of tumors/colon per mouse. Bars indicate the median with interquartile range. The number of mice with tumors out of total mice inoculated with each strain are displayed above the graph. *n* = 6 to 12 mice/group. (*Fna* denotes *F. nucleatum* subsp. *animalis*, *Fnn* denotes *F. nucleatum* subsp. *nucleatum*, *Fnv* denotes *F. nucleatum* subsp. *vincentii*, *Fnp_c* denotes clumpy *F. nucleatum* subsp. *polymorphum*, and *Fnp_nc* denotes nonclumpy *F. nucleatum* subsp. *polymorphum*).

previously shown to have proinflammatory and protumorigenic effects (Table 1) (13, 15, 30), they were also unable to significantly induce colon tumorigenesis (Fig. 3B). Surprisingly, mice persistently colonized with *F. nucleatum* were less likely to have a colon tumor (5/30 mice; 17%) than mice that cleared *F. nucleatum* (12/27 mice; 44%) (*P* = 0.04) (Fig. S4). Parallel to our findings in WT mice, there were no changes in body weight or colon length in *F. nucleatum*-colonized GF *Apc*[Min/+] mice (Fig. S5).

Evaluation of distal colon gene expression in GF *Apc*[Min/+] mice stably colonized with *F. nucleatum* by TaqMan Array, covering 45 different genes, revealed that, with the exception of nonclumpy *CRC-F. nucleatum* subsp. *polymorphum*, the CRC-derived *F. nucleatum* strains modestly but significantly upregulated expression of a number of proinflammatory cytokine and chemokine genes compared to GF control mice (Fig. 4; Table S2). There was little consistency in the genes upregulated by different CRC-derived *F. nucleatum* strains, with the exception of *Myc* (myelocytomatosis oncogene), which was upregulated by CRC-*F. nucleatum* subsp. *animalis*, CRC-*F. nucleatum* subsp. *vincentii*, and CRC-*F. nucleatum* subsp. *polymorphum*, and conversely downregulated by both non-CRC-derived *F. nucleatum* strains. Interestingly, the non-CRC strains also downregulated IL-6, IL-1β, and IL-17ra, suggesting a potential impact on type 3 immune cell function. Furthermore, histopathological analysis of GF *Apc*[Min/+] mice revealed no significant mucosal injury or inflammation; a subset of both *F. nucleatum*-colonized and control mice displayed mild reactive changes and mild crypt hyperplasia (<2×, 9/23 mice) (Fig. S5).

CRC-derived *F. nucleatum* subsp. differentially induce inflammation in a human CRC cell line *in vitro*. Because *F. nucleatum* has been shown to colonize existing human colon tumors and is hypothesized to promote CRC progression by modifying the tumor microenvironment (14), we tested the proinflammatory capacity of our CRC-derived *F. nucleatum* strains *in vitro* in the human CRC HCT116 cell line. Similar to previous findings with non-CRC-*F. nucleatum* isolates (30), our CRC- (Fig. 5) and non-CRC-derived (Fig. S6) *F. nucleatum* strains induced secretion of CXCL1 and IL-8 from HCT116 cells, although the magnitude of chemokine induction differed between strains, even within a given subspecies. While both CRC- and non-CRC-derived *F. nucleatum* subsp. *nucleatum* strains induced similar levels of chemokine secretion (CXCL1 *P* = 0.9998, IL-8 *P* = 0.9957), the CRC- and non-CRC-derived *F. nucleatum* subsp. *animalis* strains
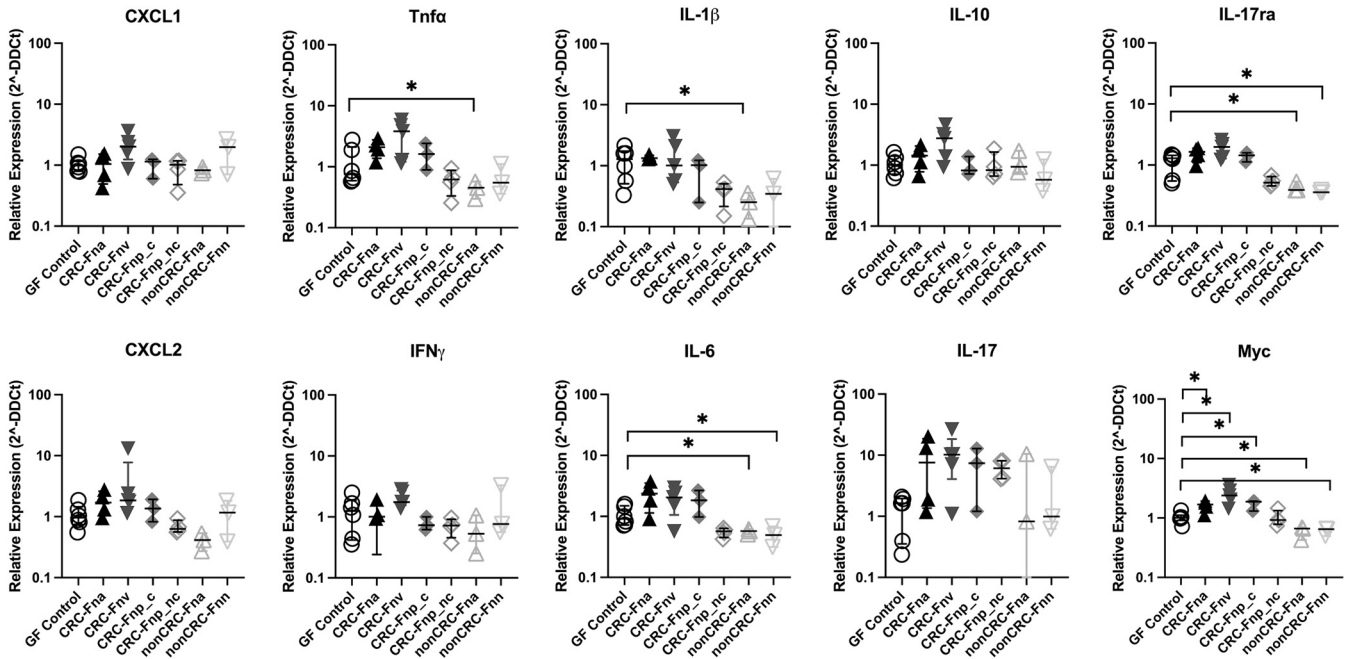
GF Min Mice

FIG 4 Changes in distal colon inflammatory gene expression in GF *Apc^{Min/+}* mice. GF *Apc^{Min/+}* mice were orally gavaged once per week for 4 weeks with the indicated strains, and distal colons were harvested at 11 weeks. Mice were only included in the analysis if they remained stably colonized for the duration of the experiment. (Therefore, strain CRC-*F. nucleatum* subsp. *nucleatum* is excluded from this figure.) Data are plotted as the relative expression ($2^{-\Delta\Delta CT}$) per mouse. Bars indicate the median with interquartile range. All P values of <0.05 were considered significant. n = 3 to 6 mice/group. (*Fna* denotes *F. nucleatum* subsp. *animalis*, *Fnn* denotes *F. nucleatum* subsp. *nucleatum*, *Fnv* denotes *F. nucleatum* subsp. *vincentii*, *Fnp_c* denotes clumpy *F. nucleatum* subsp. *polymorphum*, and *Fnp_nc* denotes nonclumpy *F. nucleatum* subsp. *polymorphum*).

significantly differed for both chemokines (P < 0.0001), with the CRC strains paradoxically inducing less chemokine expression (Fig. S6). Interestingly, the clumpy CRC-derived *F. nucleatum* subsp. *polymorphum* strain induced significantly more chemokine secretion *in vitro* than the CRC-derived nonclumpy *F. nucleatum* subsp. *polymorphum* strain (P < 0.0001). Notably, the CRC-derived *F. nucleatum* isolates that most potently
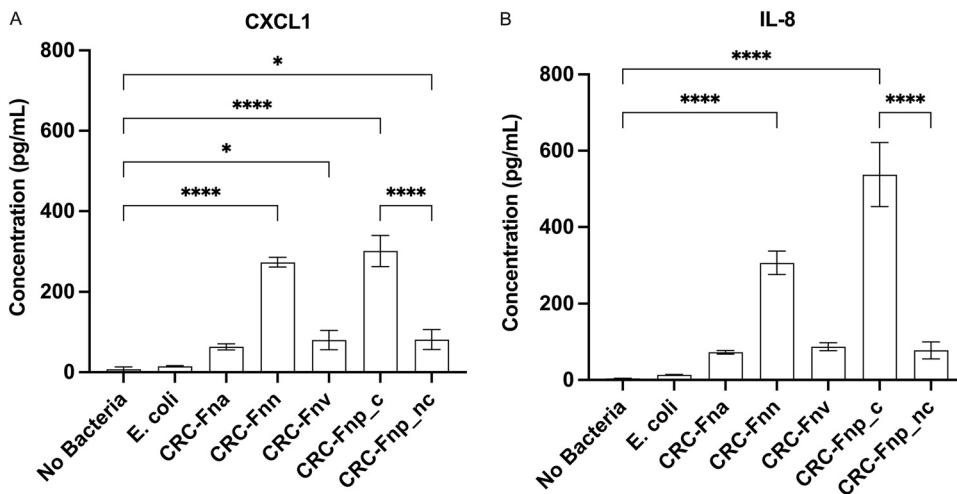
FIG 5 Secretion of CXCL1 (A) and IL-8 (B) from *F. nucleatum*-treated human HCT116 cells. HCT116 cells were incubated with *F. nucleatum* strains at an MOI of 50:1 for 4 h, and supernatants were analyzed by ELISA, performed in triplicate. Data are presented as mean ± SD. All strains depicted herein are CRC-derived isolates. For non-CRC isolates, see Fig. S6 in the supplemental material. (*Fna* denotes *F. nucleatum* subsp. *animalis*, *Fnn* denotes *F. nucleatum* subsp. *nucleatum*, *Fnv* denotes *F. nucleatum* subsp. *vincentii*, *Fnp_c* denotes clumpy *F. nucleatum* subsp. *polymorphum*, and *Fnp_nc* denotes nonclumpy *F. nucleatum* subsp. *polymorphum*).

induced secretion of CXCL1 and IL-8 from HCT116 cells were those which were least adept at colonizing our GF *Apc*^{*Min/+*} murine model (Fig. 3), highlighting the potential importance of specific host (human versus murine)-microbe interactions.

F. nucleatum subsp. differ in genome sequences and copy number of key virulence factors. Given the considerable variation in *in vitro* growth characteristics, ability to colonize our murine models, and effects on inflammatory signaling, we performed whole-genome sequencing (WGS) of our CRC-derived *F. nucleatum* strains to begin to investigate potential reasons for these varied behaviors. Eighteen previously published whole-genome sequences were included in comparative analyses (see Table S5 at https://github.com/JessicaRQueen/Queen.Domingue.mBio2022). Each of our sequenced CRC strains aligned overall with other isolates from the same subspecies regardless of clinical source (Fig. 6A). Principal-coordinate analysis (PCoA) of average nucleotide identity revealed that all sequenced *F. nucleatum* strains clustered tightly according to subspecies; within a given subspecies, strain source did not account for observed genomic variation, which was relatively minor compared to variation between subspecies (Fig. S7). Among the CRC-derived *F. nucleatum* strains, we identified a core genome consisting of 1,291 protein-coding sequences (based on an 80% identity requirement) and between 200 and 1,055 protein-coding genes unique to each individual strain (Fig. 6B).

We next evaluated all 23 complete genome sequences for the presence of several key genes encoding proteins that have been implicated as important in CRC animal models, interactions with CRC cell lines, or aggregation with other bacteria in polymicrobial biofilms (Table S1). Highly conserved *F. nucleatum* genes *recA* and *nusG* were analyzed in parallel and confirmed to be present in all 23 *F. nucleatum* strains. All sequenced *F. nucleatum* strains possessed the gene for FadA, an adhesin that binds E-cadherin, promoting cell proliferation and inflammation in a mouse xenograft model (14). There were minimal single nucleotide polymorphisms (SNPs) in *fadA*, with all strains displaying >95% *fadA* sequence identity. There are three described homologues of FadA (31), and we found that the presence of FadA2 varied between strains. As previously reported (31), FadA3 was universally present, and several *F. nucleatum* strains had multiple copies.

We also assessed for the presence of Fap2, a surface protein and galactose-binding leptin critical for colonization in the orthotopic murine model (15). Many strains lacked a *fap2* gene with high sequence homology to the *F. nucleatum* 23726 reference strain studied in the mouse model in which Fap2 mediated impairment of antitumor immunity (15). CRC-*F. nucleatum* subsp. *animalis* and clumpy CRC-*F. nucleatum* subsp. *polymorphum* had sequences with only 67% alignment with the reference Fap2 and were more closely aligned with a sequence annotated as an autotransporter-associated N-terminal domain-containing protein. It is therefore unclear if these sequences encode highly divergent Fap2 proteins or alternate proteins with a conserved autotransporter domain. Both CRC-derived *F. nucleatum* subsp. *polymorphum* strains lacked the gene for RadD, an outer membrane protein that mediates binding to other bacterial species (33–35). However, this is not unique to the *polymorphum* subspecies, as RadD is also absent in one previously sequenced *F. nucleatum* subsp. *animalis* strain (Table S1). CmpA and Aid1 are two outer membrane proteins implicated in bacterial aggregation and biofilm formation (36, 37); whereas Aid1 was present in all sequenced *F. nucleatum* strains, presence of CmpA varied, with <30% BLASTN alignment coverage to the *F. nucleatum* 23726 reference sequence in many isolates, including both *F. nucleatum* subsp. *polymorphum* strains sequenced in this study. All *F. nucleatum* strains carried the gene for FomA, a voltage-dependent porin that acts as a TLR2 agonist and has been suggested as a possible self-adjuvanted antigen for *F. nucleatum* vaccination (38). Overall, analysis of these genes hypothesized to be clinically significant failed to demonstrate any distinct characteristics of CRC-derived strains compared to non-CRC strains (Table S1).

There is little known about critical virulence factors expressed by *F. nucleatum* in the tumor microenvironment. Therefore, to identify potential additional gene products of

A

B
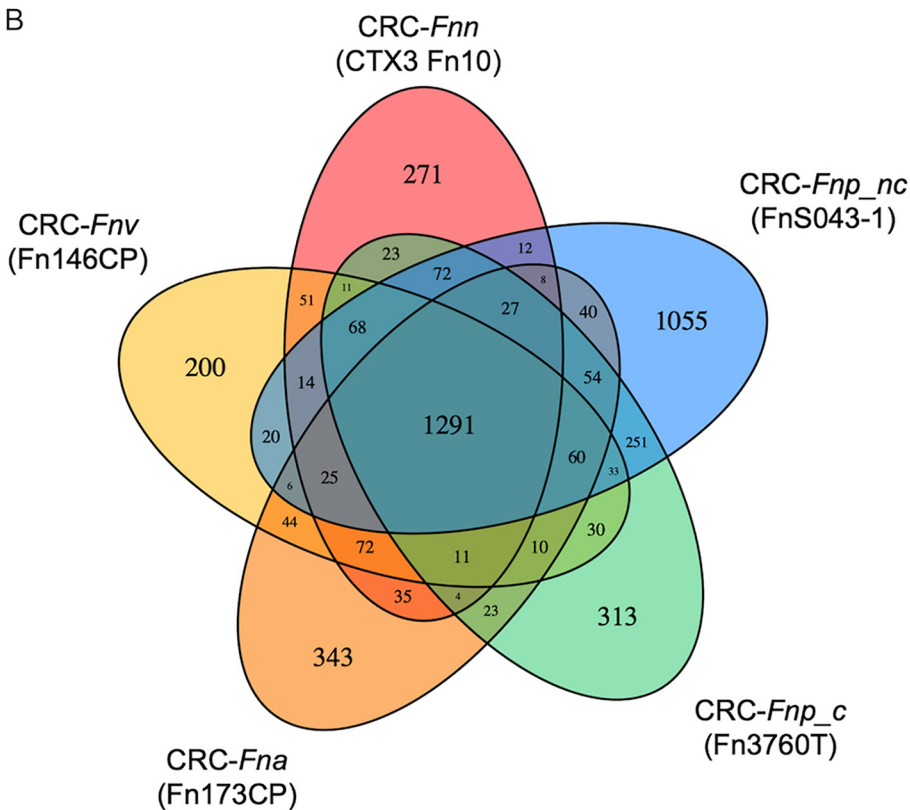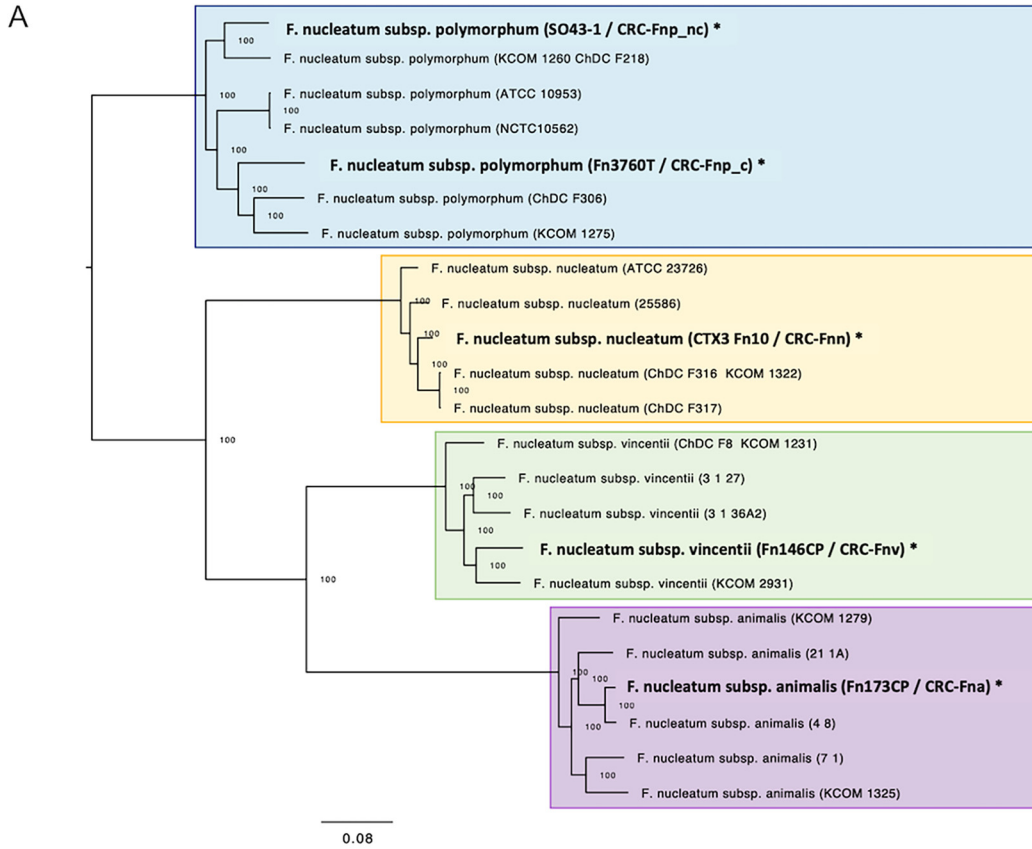
FIG 6 (A) Phylogenetic tree of 18 previously published whole-genome sequences of *F. nucleatum* strains aligned with 5 genomes newly sequenced for this study (in bold and marked with an asterisk). (B) Venn diagram depicting genomic
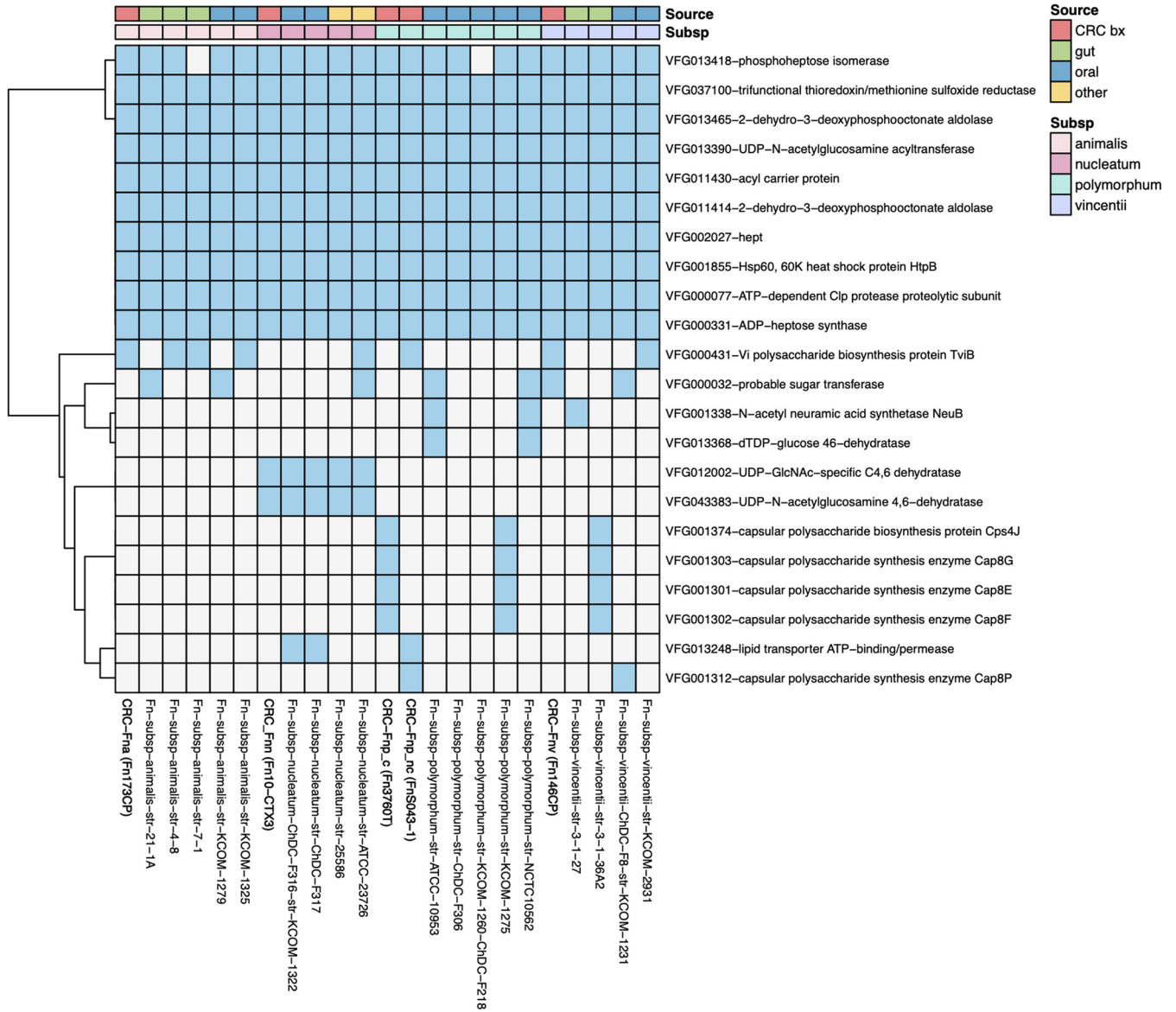
FIG 7 Heat map displaying virulence factors from the VFDB database observed in at least 2 of the 23 *F. nucleatum* isolates. Blue denotes presence, and white denotes absence. Analysis was performed on predicted protein sequences by applying BLASTP and requiring >50% amino acid identity with >85% coverage. Source of isolates (CRC biopsy specimen, gut, oral, or other) and subspecies are denoted in the color-coded legend.

clinical relevance, we performed a comparative pathogenomic analysis of *F. nucleatum* strains using the VFDB database of virulence factors expressed by pathogenic bacteria (Fig. 7) (39), which has previously been used to analyze *F. nucleatum* strains for their pathogenic potential (40). In our analysis, there were a number of gene products shared by all sequenced strains (see Table S3 at https://github.com/JessicaRQueen/Queen .Domingue.mBio2022). For example, all strains had the gene for ADP-heptose synthase, involved in generation of a lipopolysaccharide (LPS) biosynthesis pathway intermediate that has been shown to function as a pathogen-associated molecular pattern (PAMP) in

FIG 6 Legend (Continued)

comparison of the five sequenced CRC-derived *F. nucleatum* strains. Each strain is represented by a colored oval. The numbers represent the predicted protein coding genes unique to or shared by each strain, based on an 80% identity requirement. (*Fna* denotes *F. nucleatum* subsp. *animalis*, *Fnn* denotes *F. nucleatum* subsp. *nucleatum*, *Fnv* denotes *F. nucleatum* subsp. *vincentii*, *Fnp_c* denotes clumpy *F. nucleatum* subsp. *polymorphum*, and *Fnp_nc* denotes nonclumpy *F. nucleatum* subsp. *polymorphum*).

multiple Gram-negative organisms (41). A number of other genes involved in LPS biosynthesis were shared by all strains. There were no virulence genes identified unique to the CRC-derived *F. nucleatum* genomes, with the exception of nonclumpy CRC-*F. nucleatum* subsp. *polymorphum* (*F. nucleatum* S043-1), which encoded 25 virulence genes not shared by any of the 22 other *F. nucleatum* strains. This strain had >75% sequence homology to several bacterial iota toxins, including *Clostridioides difficile* transferase A and B (CdtA and CdtB) and *Clostridium perfringens* iota toxin component Ib, which ADP-ribosylates actin. This strain also possessed genes related to secretion, including general secretion pathway protein E, type IV pilus assembly protein PilB, and type VI secretion system AAA-positive (AAA⁺) family ATPase. Nonclumpy CRC-*F. nucleatum* subsp. *polymorphum* also had genes with homology to *Listeria* adhesion protein (Lap) and fibronectin-binding protein, which facilitate adherence to the intestinal epithelium. When we expanded our analysis to two additional virulence factor databases, Victors and PATRIC (42, 43), we identified numerous additional virulence genes unique to the nonclumpy CRC-*F. nucleatum* subsp. *polymorphum* strain (see Table S3 at https://github.com/JessicaRQueen/Queen.Domingue.mBio2022) and the CRC-*F. nucleatum* subsp. *vincentii* strain had a single unique virulence gene, asparagine synthetase AsnA. However, similar to the VFDB database, the Victors and PATRIC databases did not identify any gene signatures uniquely shared among the CRC-derived strains.

DISCUSSION

The association of *Fusobacterium nucleatum* with human CRC has added to our growing understanding of the critical role of the microbiota in development and progression of colon tumors, with implications for early detection, prevention, and predicting responses to therapy. It remains an open question whether *F. nucleatum* functions in the tumor microenvironment as a tumor inducer, potentiator, or merely a colonizer. Although we have convincing data from murine models that individual bacteria can induce or enhance colon tumorigenesis (e.g., enterotoxigenic *Bacteroides fragilis* and colibactin-producing *Escherichia coli*) (44, 45), it is not yet known whether putative procarcinogenic bacteria, alone or in a consortium, promote and alter tumor formation in the human colonic microenvironment. Microbiota dysbiosis and resultant inflammation are hypothesized to drive carcinogenesis (46). In contrast, available data on the contributions of *F. nucleatum* to CRC pathogenesis from murine models is limited and of uncertain validity because a stable colonization model, which mimics the anticipated condition in humans, has not yet been reported. Daily gavage of an organism in mice may represent an antigen stimulation model leading to the low-level colon tumorigenesis reported to date. In prior studies, daily *F. nucleatum* inoculation was associated with NF-κB activation (13), which we speculate may have promoted the modest tumor induction reported through a nonspecific response to repeated exposure to LPS and other Gram-negative PAMPs.

Herein, we sought first to test potential conditions in SPF mice that are expected to yield stable colonization. However, despite repeated gavages of *F. nucleatum*, neither persistent colonization nor tumorigenesis was observed. One possibility for the difficulty of establishing a robust SPF murine model for *F. nucleatum* colon tumorigenesis is that mice are not a natural host of *F. nucleatum*, which may be a highly human-adapted organism. Thus, mouse colon epithelial and/or immune cells may lack critical receptors for *F. nucleatum* adhesion factors that are essential for persistent colonization. For example, Fap2 expressed by *F. nucleatum* binds to human, but not murine, TIGIT, an inhibitory receptor that suppresses antitumor immunity (47). Our data indicate that SPF mice have a high resistance to colonization despite reduction of the microbiota with broad-spectrum antibiotics and repeated *F. nucleatum* inoculations. Although we could successfully colonize GF mice after multiple inoculations, many were ultimately able to clear *F. nucleatum*, suggesting even the less developed GF mouse immune system can eliminate *F. nucleatum* from the murine colon. In addition, although we hypothesized that *F. nucleatum* would induce colon biofilms given its

well-described role as a facilitator of polymicrobial biofilm formation and maturation in the oral mucosa, *F. nucleatum* biofilms were not observed in well-colonized GF WT mice.

Further, our studies in the GF *Apc^{Min/+}* model of CRC suggest that colonization with *F. nucleatum* alone is insufficient to induce formation of colonic tumors and suggests that, unexpectedly, persistent *F. nucleatum* colonization may exert an antitumor effect. This lack of tumor induction by *F. nucleatum* was observed across all subspecies tested despite variable modest distal colon inflammatory gene expression not accompanied by histopathologic inflammation. These data suggest that if *F. nucleatum* subspecies induce colon tumorigenesis, this may require a specific consortium of cross-communicating or synergistic bacteria. Our data demonstrating a lack of tumor induction by *F. nucleatum* in the GF *Apc^{MinΔ716/+}* mouse model are supported by an earlier study in which GF *Apc^{MinΔ850/+}* mice were administered a weekly gavage of a human CRC-derived *F. nucleatum* isolate or a combination of 6 *F. nucleatum* isolates from subsp. *animalis*, *nucleatum*, and *vincentii* (28). In parallel studies, *F. nucleatum* was gavaged following administration of an intact SPF microbiota. After 20 weeks, mice in all groups were assessed, and no significant intestinal tumorigenesis was observed.

In contrast, our studies and others in human-derived CRC cell lines suggest that when human tumor cells are present, some strains of *F. nucleatum* can be potent inducers of proinflammatory cytokines that are known to promote tumor cell migration and invasion (30). Herein, we demonstrate that *F. nucleatum* strains, across subspecies, can promote inflammatory signaling in a human colon cancer cell line; however, the magnitude of inflammation varied between isolates. These data highlight that *F. nucleatum* strains isolated from colonic tumors and other clinical specimens differ in their ability to promote inflammation *in vitro* and possibly in the human host. Given the weak *F. nucleatum* phenotypes in mouse models, further studies of humans with CRC with and without *F. nucleatum* colonization are needed to understand the contribution of *F. nucleatum* to human colon carcinogenesis.

Although sequencing analysis has demonstrated an enrichment of *F. nucleatum* in the tumor-associated microbiota of a proportion of CRC patients (7, 13), we lack a clear understanding of which subspecies are most relevant. *F. nucleatum* subspecies can be differentiated biochemically and genomically (2, 48). Based on average nucleotide identity or genome-to-genome analysis of whole-genome sequences, it has recently been suggested that there is sufficient genetic heterogeneity between the subspecies that they should be reclassified as separate species (49). Analysis of cancer-associated microbiota that relies on partial sequencing of the 16S rRNA gene lacks the resolution to identify the *F. nucleatum* subspecies in clinical samples. Therefore, sequencing paired with culture methods to isolate and further characterize specific *F. nucleatum* strains is needed. A novel PCR-based method for distinguishing the *F. nucleatum* subsp. was recently reported (50); validation of this promising technique in geographically diverse patient samples will be helpful given our findings of significant sequence variation in our nonclumpy CRC-*F. nucleatum* subsp. *polymorphum* strain collected in Malaysia compared to clinical isolates from Western Europe and the United States.

The limited number of fully sequenced *F. nucleatum* genomes indicates a high degree of genetic variation between strains. Our whole-genome sequencing analysis supports this, with CRC-derived strains clustering with other isolates from the same subspecies, but with significant variability in genes encoding proteins that have been implicated in existing CRC animal models. In particular, we observed significant variation in Fap2, where it is either absent or highly divergent in several *F. nucleatum* isolates. Furthermore, we identified several virulence genes unique to just the nonclumpy CRC-*F. nucleatum* subsp. *polymorphum* strain. It is possible that the high degree of divergence observed in this strain reflects geographic diversity, as this was the only CRC-derived strain in our cohort isolated in Asia. Previous genomic analysis of the *F. nucleatum* subsp. *polymorphum* strain ATCC 10953 revealed that 25% of the protein-coding genes were unique to that strain, with evidence of horizontal gene transfer

with *Firmicutes*, particularly *Clostridia* (51). It is unclear whether this genetic tractability is unique to *F. nucleatum* subsp. *polymorphum* or if this is a strain-specific property. Further studies will be necessary to assess expression and function of *F. nucleatum* genes of interest in various experimental conditions.

In conclusion, we have demonstrated that stable colonization of GF *Apc^{Min/+}* mice with CRC-derived *F. nucleatum* may modestly modulate host immune responses but does not promote colonic tumor formation in a monocolonized gnotobiotic mouse model. Behavior of *F. nucleatum* isolates in both *in vitro* and *in vivo* assays differed at the subspecies and strain levels, but there was no clear genomic distinction between tumor-associated *F. nucleatum* isolates and other clinical strains. We hypothesize that *F. nucleatum* may act in concert with other bacteria to activate essential carcinogenic signaling and promote formation or progression of colon tumors. However, differences in human and murine immune signaling may account for the lack of tumor promotion in mouse models.

Future studies on the role of *F. nucleatum* in colonic tumorigenesis will benefit from development of robust, persistently colonized animal models of CRC that examine *F. nucleatum* in association with other members of the colon and oral microbiota that are enriched in colonic tumors. Examination of subspecies- and strain-specific phenotypes in robust *F. nucleatum* models, with particular emphasis on investigation of CRC-derived clinical isolates, will be critical to further define the role of *F. nucleatum* in colon tumorigenesis and to delineate mechanisms of pathogenesis.

MATERIALS AND METHODS

Culturing and inoculum preparation. *F. nucleatum* strains used in this study (Table 1) were either previously isolated from CRC biopsy tissue or other clinical sites and obtained from the sources listed in Table 1 or were isolated for this study from human CRC biopsy specimens using selective culture media (*Fusobacterium* selective agar; Anaerobe Systems) and identified by colony PCR with *Fusobacterium*-specific 16S primers (forward, 5'-GGATTTATTGGGCGTAAAG-3'C; reverse, 5'-GGCATTCCTACAAATATCTACGAA-3') (52), and the species and subspecies were confirmed by Sanger sequencing of the 16S rRNA gene. *F. nucleatum* strains were cultured in brain heart infusion (BHI) media supplemented with hemin (10 μg/mL) and vitamin K (5 μg/mL) under anaerobic conditions (75% N_2, 5% H_2, 20% CO_2) at 37°C for 48 to 72 h in static culture (to an optical density at 600 nm [OD_{600}] of ~1.5). Bacterial cultures were centrifuged and pellets resuspended in phosphate-buffered saline (PBS) under anaerobic conditions prior to animal inoculation.

Murine models. Wild-type C57BL/6J (WT; Jackson Laboratories) and multiple intestinal neoplasia mice (*Apc^{MinΔ716/+}*, more permissive to intestinal tumorigenesis than *Apc^{MinΔ850/+}* mice [53], termed *Apc^{Min/+}* here; from David Huso, Johns Hopkins University) were housed in either the specific-pathogen-free (SPF) or germfree (GF) barrier facilities, as indicated. Six- to 10-week-old male and female mice were used for all experiments. Mice were maintained on a 12-h light/dark cycle and fed standard rodent chow *ad libitum*. For SPF experiments, we used two approaches. In the first, WT mice were treated with cefoxitin (5 mg/mL) *ad libitum* in drinking water for 48 h and then supplied with normal water for 36 h prior to the first inoculation; this approach was previously shown to temporarily eliminate detectable gut bacteria (54). Mice were maintained on gentamicin (35 μg/mL) *ad libitum* in drinking water for the duration of the experiment to further foster a dysbiotic microbiota potentially permissive to *Fusobacterium* spp. colonization. Antibiotic-treated SPF WT mice were inoculated via orogastric administration with 200 μL of *F. nucleatum* inoculum (equivalent to ~10^9 genome copies) once weekly for 4 weeks. In our second approach, SPF *Apc^{Min/+}* mice were treated with streptomycin (5 mg/mL) and clindamycin (0.1 mg/mL) *ad libitum* in drinking water for 5 days prior to the first inoculation with normal water provided for the experiment duration. These mice were treated with an intensified gavage scheme of orogastric inoculum gavage three times in the first week, followed by weekly gavage for 10 weeks.

GF WT and *Apc^{Min/+}* mice were inoculated in a laminar flow hood via orogastric gavage with 200 μL of *F. nucleatum* inoculum once weekly for 4 weeks, except for 2-week-long experiments where *F. nucleatum* was administered once. Individual GF cages (Allentown, Inc., NJ) were used for each experimental group to prevent cross-contamination of *F. nucleatum* strains. Mice were euthanized at the indicated time points and tissues harvested for further analyses. Fecal *F. nucleatum* colonization was assessed via reverse transcription-quantitative PCR (qRT-PCR) analysis of the *Fusobacterium* 16S rRNA gene. Distal colon gene expression was assessed by qRT-PCR using TaqMan gene expression assays, and each target gene was normalized to murine GAPDH (glyceraldehyde-3-phosphate dehydrogenase) and/or GusB. Downstream processing of mouse stools and tissues is further described in Text S1 in the supplemental material. The Johns Hopkins University Animal Care and Use Committee approved all experimental protocols, and all studies were in accordance with Animal Research: Reporting of *In Vivo* Experiments (ARRIVE) guidelines.

***In vitro* cytokine release assay.** As previously described (30), HCT116 (ATCC CCL-247) cells were grown on tissue culture-treated plates and flasks in McCoy's 5A medium supplemented with 10% fetal

bovine serum (FBS), penicillin, and streptomycin. HCT116 cells were seeded to confluence in 24-well plates (2×10^5 cells per well at 100% confluence), and *F. nucleatum* subspecies were added at a multiplicity of infection (MOI) of 50:1 followed by incubation at 37°C and 5% CO_2 for 4 h. Medium from individual wells was sterile filtered using a 0.2-μm filter (MilliporeSigma) and diluted to concentrations within the range of the R&D Systems DuoSet enzyme-linked immunosorbent assay (ELISA) to analyze human IL-8 and CXCL1 concentrations.

WGS and comparative genome analysis. WGS was done at the PennCHOP Microbiome Center (University of Pennsylvania) using Illumina MiSeq technology as described in Text S1. WGS data sets were trimmed for quality using FASTP v0.20.0 (55), assembled using SPAdes v3.14.1 (56), and annotated for gene content using the DFAST pipeline v1.2.6 (57) and PROKKA v1.14.5 (58), followed by MetaCyc pathway analysis with MinPath (59). Genome sequences of the 5 newly sequenced CRC-derived *F. nucleatum* strains were compared to 18 previously sequenced complete genomes, all of which were non-CRC-derived isolates and were inclusive of strains *F. nucleatum* 23726 and *F. nucleatum* EAVG_002 described in Table 1. Whole-genome alignment of sequenced and reference *Fusobacterium* isolates was performed using MUGSY v1r2.3 (60). Core alignment blocks ($\geq$1,000 bp) covering all considered strains were concatenated into a larger alignment (totaling 1,362,030 bp). This alignment was narrowed to positions containing SNPs (n = 240,340) and submitted to FastTree v1 (61) for phylogenetic tree construction. To study whole-genome variation between and within subspecies and by source, the concatenated whole-genome alignment was used to calculate average nucleotide identity (ANI) between all strains counting SNP-based mismatches that were observed $\geq$100 bp from the end of each original core alignment block. ANI measures were then converted to a dissimilarity matrix, followed by principal-coordinate analysis (PCoA) and permutational multivariate analysis of variance (PERMANOVA) using the Vegan R package v2.5.6. To evaluate shared and unique gene content, coding sequences from each of the five *F. nucleatum* isolates were clustered using USEARCH v11.0.667 (62) with an 80% identity threshold and visualization of overlapping membership per cluster by VennDiagram in R v3.5.3. Virulence factor searches were performed on predicted protein sequences of 23 *F. nucleatum* strains using the PATRIC (42), Victors (43), and VFDB (39) databases by applying BLASTP and requiring >50% amino acid identity with >85% coverage. VFDB categories with at least two positive calls based on identity and coverage criteria were analyzed as binary data for heatmap generation using the pheatmap R package (v1.0.12) and specifying the Manhattan distance to cluster virulence factor categories. Nondefault parameter settings for all computational analyses are available in Table S4 at https://github.com/JessicaRQueen/Queen.Domingue.mBio2022. Name, accession number, and clinical source for the 18 previously sequenced strains and the 5 strains sequenced for this study are listed in Table S5 at https://github.com/JessicaRQueen/Queen.Domingue.mBio2022.

Statistical analysis. For colonization analyses, murine groups were analyzed using a Mann-Whitney (nonparametric) test. For comparative analysis of gene expression levels and tumorigenesis, we performed a nonparametric Kruskal-Wallis one-way ANOVA; significant pairwise comparisons were subsequently analyzed by Mann-Whitney test. Linear regression was performed for correlation of gene expression and *F. nucleatum* copy number (analyzed by qRT-PCR as described in Text S1 at https://github.com/JessicaRQueen/Queen.Domingue.mBio2022). Fisher's exact test was performed for comparison of tumorigenesis in *F. nucleatum*-colonized versus cleared mice. Results from *in vitro* assays were analyzed by parametric one-way ANOVA with Tukey's test for multiple comparisons. Differences with a *P* value of <0.05 were considered significant.

Data availability. Whole-genome sequencing data have been submitted to NCBI under NCBI BioProject accession ID PRJNA755318. Accession numbers for the 5 strains sequenced for this work as are follows: for Fn146CP, SAMN20819806; for Fn173CP, SAMN20819807; for CTX3Fn10, SAMN20819805; for Fn3760T, SAMN20819808; and for FnS043-1, SAMN20819809.

SUPPLEMENTAL MATERIAL

Supplemental material is available online only.

TEXT S1, DOCX file, 0.03 MB.
FIG S1, TIF file, 0.3 MB.
FIG S2, TIF file, 2.6 MB.
FIG S3, TIF file, 2.8 MB.
FIG S4, TIF file, 0.1 MB.
FIG S5, TIF file, 0.4 MB.
FIG S6, TIF file, 0.1 MB.
FIG S7, TIF file, 2.3 MB.
TABLE S1, PDF file, 0.02 MB.
TABLE S2, PDF file, 0.1 MB.

ACKNOWLEDGMENTS

REFERENCES

1. Han YW. 2015. Fusobacterium nucleatum: a commensal-turned patho-gen. Curr Opin Microbiol 23:141–147. https://doi.org/10.1016/j.mib.2014.11.013.

2. Gharbia SE, Shah HN. 1990. Identification of Fusobacterium species by the electrophoretic migration of glutamate dehydrogenase and 2-oxo-glutarate reductase in relation to their DNA base composition and pepti-doglycan dibasic amino acids. J Med Microbiol 33:183–188. https://doi.org/10.1099/00222615-33-3-183.

3. Li Y, Guo H, Wang X, Lu Y, Yang C, Yang P. 2015. Coinfection with Fuso-bacterium nucleatum can enhance the attachment and invasion of Por-phyromonas gingivalis or Aggregatibacter actinomycetemcomitans to human gingival epithelial cells. Arch Oral Biol 60:1387–1393. https://doi.org/10.1016/j.archoralbio.2015.06.017.

4. Okuda T, Kokubu E, Kawana T, Saito A, Okuda K, Ishihara K. 2012. Synergy in biofilm formation between Fusobacterium nucleatum and Prevotella species. Anaerobe 18:110–116. https://doi.org/10.1016/j.anaerobe.2011.09.003.

5. Metzger Z, Blasbalg J, Dotan M, Weiss EI. 2009. Enhanced attachment of Porphyromonas gingivalis to human fibroblasts mediated by Fusobacte-rium nucleatum. J Endod 35:82–85. https://doi.org/10.1016/j.joen.2008.10.011.

6. Gharbia SE, Shah HN. 1992. Fusobacterium nucleatum subsp. fusiforme subsp. nov. and Fusobacterium nucleatum subsp. animalis subsp. nov. as additional subspecies within Fusobacterium nucleatum. Int J Syst Bacter-iol 42:296–298. https://doi.org/10.1099/00207713-42-2-296.

7. Castellarin M, Warren RL, Freeman JD, Dreolini L, Krzywinski M, Strauss J, Barnes R, Watson P, Allen-Vercoe E, Moore RA, Holt RA. 2012. Fusobacte-rium nucleatum infection is prevalent in human colorectal carcinoma. Ge-nome Res 22:299–306. https://doi.org/10.1101/gr.126516.111.

8. Kostic AD, Gevers D, Pedamallu CS, Michaud M, Duke F, Earl AM, Ojesina AI, Jung J, Bass AJ, Tabernero J, Baselga J, Liu C, Shivdasani RA, Ogino S, Birren BW, Huttenhower C, Garrett WS, Meyerson M. 2012. Genomic anal-ysis identifies association of Fusobacterium with colorectal carcinoma. Genome Res 22:292–298. https://doi.org/10.1101/gr.126573.111.

9. Repass J, Iorns E, Denis A, Williams SR, Perfito N, Errington TM, Reproduci-bility Project: Cancer Biology. 2018. Replication study: Fusobacterium nucleatum infection is prevalent in human colorectal carcinoma. Elife 7: e25801. https://doi.org/10.7554/eLife.25801.

10. Mima K, Cao Y, Chan AT, Qian ZR, Nowak JA, Masugi Y, Shi Y, Song M, da Silva A, Gu M, Li W, Hamada T, Kosumi K, Hanyuda A, Liu L, Kostic AD, Giannakis M, Bullman S, Brennan CA, Milner DA, Baba H, Garraway LA, Meyerhardt JA, Garrett WS, Huttenhower C, Meyerson M, Giovannucci EL, Fuchs CS, Nishihara R, Ogino S. 2016. Fusobacterium nucleatum in colo-rectal carcinoma tissue according to tumor location. Clin Transl Gastroen-terol 7:e200. https://doi.org/10.1038/ctg.2016.53.

11. Li YY, Ge QX, Cao J, Zhou YJ, Du YL, Shen B, Wan YJ, Nie YQ. 2016. Associa-tion of Fusobacterium nucleatum infection with colorectal cancer in Chi-nese patients. WJG 22:3227–3233. https://doi.org/10.3748/wjg.v22.i11.3227.

12. Marchesi JR, Dutilh BE, Hall N, Peters WH, Roelofs R, Boleij A, Tjalsma H. 2011. Towards the human colorectal cancer microbiome. PLoS One 6: e20447. https://doi.org/10.1371/journal.pone.0020447.

13. Kostic AD, Chun E, Robertson L, Glickman JN, Gallini CA, Michaud M, Clancy TE, Chung DC, Lochhead P, Hold GL, El-Omar EM, Brenner D, Fuchs CS, Meyerson M, Garrett WS. 2013. Fusobacterium nucleatum potentiates intestinal tumorigenesis and modulates the tumor-immune microenvir-onment. Cell Host Microbe 14:207–215. https://doi.org/10.1016/j.chom.2013.07.007.

14. Rubinstein MR, Wang X, Liu W, Hao Y, Cai G, Han YW. 2013. Fusobacte-rium nucleatum promotes colorectal carcinogenesis by modulating E-cadherin/β-catenin signaling via its FadA adhesin. Cell Host Microbe 14: 195–206. https://doi.org/10.1016/j.chom.2013.07.012.

15. Abed J, Emgård JE, Zamir G, Faroja M, Almogy G, Grenov A, Sol A, Naor R, Pikarsky E, Atlan KA, Mellul A, Chaushu S, Manson AL, Earl AM, Ou N, Brennan CA, Garrett WS, Bachrach G. 2016. Fap2 Mediates Fusobacterium nucleatum colorectal adenocarcinoma enrichment by binding to tumor-expressed Gal-GalNAc. Cell Host Microbe 20:215–225. https://doi.org/10.1016/j.chom.2016.07.006.

16. Yang Y, Weng W, Peng J, Hong L, Yang L, Toiyama Y, Gao R, Liu M, Yin M, Pan C, Li H, Guo B, Zhu Q, Wei Q, Moyer MP, Wang P, Cai S, Goel A, Qin H, Ma Y. 2017. Fusobacterium nucleatum increases proliferation of colo-rectal cancer cells and tumor development in mice by activating Toll-like receptor 4 signaling to nuclear factor-κB, and up-regulating expression of microRNA-21. Gastroenterology 152:851–866.e24. https://doi.org/10.1053/j.gastro.2016.11.018.

17. Bullman S, Pedamallu CS, Sicinska E, Clancy TE, Zhang X, Cai D, Neuberg D, Huang K, Guevara F, Nelson T, Chipashvili O, Hagan T, Walker M, Ramachandran A, Diosdado B, Serna G, Mulet N, Landolfi S, Ramon Y Cajal S, Fasani R, Aguirre AJ, Ng K, Élez E, Ogino S, Tabernero J, Fuchs CS, Hahn WC, Nuciforo P, Meyerson M. 2017. Analysis of Fusobacterium per-sistence and antibiotic response in colorectal cancer. Science 358: 1443–1448. https://doi.org/10.1126/science.aal5240.

18. Yu YN, Yu TC, Zhao HJ, Sun TT, Chen HM, Chen HY, An HF, Weng YR, Yu J, Li M, Qin WX, Ma X, Shen N, Hong J, Fang JY. 2015. Berberine may rescue Fusobacterium nucleatum-induced colorectal tumorigenesis by modulat-ing the tumor microenvironment. Oncotarget 6:32013–32026. https://doi.org/10.18632/oncotarget.5166.

19. Yu T, Guo F, Yu Y, Sun T, Ma D, Han J, Qian Y, Kryczek I, Sun D, Nagarsheth N, Chen Y, Chen H, Hong J, Zou W, Fang JY. 2017. Fusobacterium nuclea-tum promotes chemoresistance to colorectal cancer by modulating autophagy. Cell 170:548–563.e16. https://doi.org/10.1016/j.cell.2017.07.008.

20. Chen Y, Peng Y, Yu J, Chen T, Wu Y, Shi L, Li Q, Wu J, Fu X. 2017. Invasive Fusobacterium nucleatum activates beta-catenin signaling in colorectal cancer via a TLR4/P-PAK1 cascade. Oncotarget 8:31802–31814. https://doi.org/10.18632/oncotarget.15992.

21. Abed J, Maalouf N, Manson AL, Earl AM, Parhi L, Emgård JEM, Klutstein M, Tayeb S, Almogy G, Atlan KA, Chaushu S, Israeli E, Mandelboim O, Garrett WS, Bachrach G. 2020. Colon cancer-associated *Fusobacterium nucleatum* may originate from the oral cavity and reach colon tumors via the

circulatory system. Front Cell Infect Microbiol 10:400. https://doi.org/10.3389/fcimb.2020.00400.

22. Ye X, Wang R, Bhattacharya R, Boulbes DR, Fan F, Xia L, Adoni H, Ajami NJ, Wong MC, Smith DP, Petrosino JF, Venable S, Qiao W, Baladandayuthapani V, Maru D, Ellis LM. 2017. Fusobacterium nucleatum subspecies animalis influences proinflammatory cytokine expression and monocyte activation in human colorectal tumors. Cancer Prev Res (Phila) 10:398–409. https://doi.org/10.1158/1940-6207.CAPR-16-0178.

23. Wu Y, Wu J, Chen T, Li Q, Peng W, Li H, Tang X, Fu X. 2018. Fusobacterium nucleatum potentiates intestinal tumorigenesis in mice via a Toll-like receptor 4/p21-activated kinase 1 cascade. Dig Dis Sci 63:1210–1218. https://doi.org/10.1007/s10620-018-4999-2.

24. Guo P, Tian Z, Kong X, Yang L, Shan X, Dong B, Ding X, Jing X, Jiang C, Jiang N, Yu Y. 2020. FadA promotes DNA damage and progression of Fusobacterium nucleatum-induced colorectal cancer through up-regulation of chk2. J Exp Clin Cancer Res 39:202. https://doi.org/10.1186/s13046-020-01677-w.

25. Rhee KJ, Wu S, Wu X, Huso DL, Karim B, Franco AA, Rabizadeh S, Golub JE, Mathews LE, Shin J, Sartor RB, Golenbock D, Hamad AR, Gan CM, Housseau F, Sears CL. 2009. Induction of persistent colitis by a human commensal, enterotoxigenic Bacteroides fragilis, in wild-type C57BL/6 mice. Infect Immun 77:1708–1718. https://doi.org/10.1128/IAI.00814-08.

26. DeStefano Shields CE, White JR, Chung L, Wenzel A, Hicks JL, Tam AJ, Chan JL, Dejea CM, Fan H, Michel J, Maiuri AR, Sriramkumar S, Podicheti R, Rusch DB, Wang H, DeMarzo AM, Huso DL, Besharati S, Anders RA, Baylin SB, O'Hagan HM, Housseau F, Sears CL. 2017. Bacterial-driven inflammation and mutant BRAF expression combine to promote murine colon tumorigenesis that is sensitive to immune checkpoint therapy. Cancer Discov 11:1792–1807. https://doi.org/10.1158/2159-8290.CD-20-0770.

27. Drewes JL, White JR, Dejea CM, Fathi P, Iyadorai T, Vadivelu J, Roslani AC, Wick EC, Mongodin EF, Loke MF, Thulasi K, Gan HM, Goh KL, Chong HY, Kumar S, Wanyiri JW, Sears CL. 2017. High-resolution bacterial 16S rRNA gene profile meta-analysis and biofilm status reveal common colorectal cancer consortia. NPJ Biofilms Microbiomes 3:34. https://doi.org/10.1038/s41522-017-0040-3.

28. Tomkovich S, Yang Y, Winglee K, Gauthier J, Mühlbauer M, Sun X, Mohamadzadeh M, Liu X, Martin P, Wang GP, Oswald E, Fodor AA, Jobin C. 2017. Locoregional effects of microbiota in a preclinical model of colon carcinogenesis. Cancer Res 77:2620–2632. https://doi.org/10.1158/0008-5472.CAN-16-3472.

29. Terzić J, Grivennikov S, Karin E, Karin M. 2010. Inflammation and colon cancer. Gastroenterology 138:2101–2114.e5. https://doi.org/10.1053/j.gastro.2010.01.058.

30. Casasanta MA, Yoo CC, Udayasuryan B, Sanders BE, Umaña A, Zhang Y, Peng H, Duncan AJ, Wang Y, Li L, Verbridge SS, Slade DJ. 2020. Fusobacterium nucleatum host-cell binding and invasion induces IL-8 and CXCL1 secretion that drives colorectal cancer cell migration. Sci Signal 13:eaba9157. https://doi.org/10.1126/scisignal.aba9157.

31. Umaña A, Sanders BE, Yoo CC, Casasanta MA, Udayasuryan B, Verbridge SS, Slade DJ. 2019. Utilizing whole Fusobacterium genomes to identify, correct, and characterize potential virulence protein families. J Bacteriol 201:e00273-19. https://doi.org/10.1128/JB.00273-19.

32. Reference deleted.

33. Kaplan CW, Lux R, Haake SK, Shi W. 2009. The Fusobacterium nucleatum outer membrane protein RadD is an arginine-inhibitable adhesin required for inter-species adherence and the structured architecture of multispecies biofilm. Mol Microbiol 71:35–47. https://doi.org/10.1111/j.1365-2958.2008.06503.x.

34. Engevik MA, Danhof HA, Auchtung J, Endres BT, Ruan W, Bassères E, Engevik AC, Wu Q, Nicholson M, Luna RA, Garey KW, Crawford SE, Estes MK, Lux R, Yacyshyn MB, Yacyshyn B, Savidge T, Britton RA, Versalovic J. 2021. Fusobacterium nucleatum adheres to Clostridioides difficile via the RadD adhesin to enhance biofilm formation in intestinal mucus. Gastroenterology 160:1301–1314.e8. https://doi.org/10.1053/j.gastro.2020.11.034.

35. Guo L, Shokeen B, He X, Shi W, Lux R. 2017. Streptococcus mutans SpaP binds to RadD of Fusobacterium nucleatum ssp. polymorphum. Mol Oral Microbiol 32:355–364. https://doi.org/10.1111/omi.12177.

36. Kaplan A, Kaplan CW, He X, McHardy I, Shi W, Lux R. 2014. Characterization of aid1, a novel gene involved in Fusobacterium nucleatum interspecies interactions. Microb Ecol 68:379–387. https://doi.org/10.1007/s00248-014-0400-y.

37. Lima BP, Shi W, Lux R. 2017. Identification and characterization of a novel Fusobacterium nucleatum adhesin involved in physical interaction and biofilm formation with Streptococcus gordonii. Microbiologyopen 6:e00444. https://doi.org/10.1002/mbo3.444.

38. Toussi DN, Liu X, Massari P. 2012. The FomA porin from Fusobacterium nucleatum is a Toll-like receptor 2 agonist with immune adjuvant activity. Clin Vaccine Immunol 19:1093–1101. https://doi.org/10.1128/CVI.00236-12.

39. Chen L, Yang J, Yu J, Yao Z, Sun L, Shen Y, Jin Q. 2005. VFDB: a reference database for bacterial virulence factors. Nucleic Acids Res 33:D325–D328. https://doi.org/10.1093/nar/gki008.

40. Ang MY, Dutta A, Wee WY, Dymock D, Paterson IC, Choo SW. 2016. Comparative genome analysis of Fusobacterium nucleatum. Genome Biol Evol 8:2928–2938. https://doi.org/10.1093/gbe/evw199.

41. García-Weber D, Arrieumerlou C. 2021. ADP-heptose: a bacterial PAMP detected by the host sensor ALPK1. Cell Mol Life Sci 78:17–29. https://doi.org/10.1007/s00018-020-03577-w.

42. Brettin T, Davis JJ, Disz T, Edwards RA, Gerdes S, Olsen GJ, Olson R, Overbeek R, Parrello B, Pusch GD, Shukla M, Thomason JA, Stevens R, Vonstein V, Wattam AR, Xia F. 2015. RASTtk: a modular and extensible implementation of the RAST algorithm for building custom annotation pipelines and annotating batches of genomes. Sci Rep 5:8365. https://doi.org/10.1038/srep08365.

43. Sayers S, Li L, Ong E, Deng S, Fu G, Lin Y, Yang B, Zhang S, Fa Z, Zhao B, Xiang Z, Li Y, Zhao XM, Olszewski MA, Chen L, He Y. 2019. Victors: a web-based knowledge base of virulence factors in human and animal pathogens. Nucleic Acids Res 47:D693–D700. https://doi.org/10.1093/nar/gky999.

44. Arthur JC, Perez-Chanona E, Mühlbauer M, Tomkovich S, Uronis JM, Fan TJ, Campbell BJ, Abujamel T, Dogan B, Rogers AB, Rhodes JM, Stintzi A, Simpson KW, Hansen JJ, Keku TO, Fodor AA, Jobin C. 2012. Intestinal inflammation targets cancer-inducing activity of the microbiota. Science 338:120–123. https://doi.org/10.1126/science.1224820.

45. Wu S, Rhee KJ, Albesiano E, Rabizadeh S, Wu X, Yen HR, Huso DL, Brancati FL, Wick E, McAllister F, Housseau F, Pardoll DM, Sears CL. 2009. A human colonic commensal promotes colon tumorigenesis via activation of T helper type 17 T cell responses. Nat Med 15:1016–1022. https://doi.org/10.1038/nm.2015.

46. Chen J, Domingue JC, Sears CL. 2017. Microbiota dysbiosis in select human cancers: evidence of association and causality. Semin Immunol 32:25–34. https://doi.org/10.1016/j.smim.2017.08.001.

47. Gur C, Ibrahim Y, Isaacson B, Yamin R, Abed J, Gamliel M, Enk J, Bar-On Y, Stanietsky-Kaynan N, Coppenhagen-Glazer S, Shussman N, Almogy G, Cuapio A, Hofer E, Mevorach D, Tabib A, Ortenberg R, Markel G, Miklić K, Jonjic S, Brennan CA, Garrett WS, Bachrach G, Mandelboim O. 2015. Binding of the Fap2 protein of Fusobacterium nucleatum to human inhibitory receptor TIGIT protects tumors from immune cell attack. Immunity 42:344–355. https://doi.org/10.1016/j.immuni.2015.01.010.

48. Kim HS, Lee DS, Chang YH, Kim MJ, Koh S, Kim J, Seong JH, Song SK, Shin HS, Son JB, Jung MY, Park SN, Yoo SY, Cho KW, Kim DK, Moon S, Kim D, Choi Y, Kim BO, Jang HS, Kim CS, Kim C, Choe SJ, Kook JK. 2010. Application of rpoB and zinc protease gene for use in molecular discrimination of Fusobacterium nucleatum subspecies. J Clin Microbiol 48:545–553. https://doi.org/10.1128/JCM.01631-09.

49. Kook JK, Park SN, Lim YK, Cho E, Jo E, Roh H, Shin Y, Paek J, Kim HS, Kim H, Shin JH, Chang YH. 2017. Genome-based reclassification of Fusobacterium nucleatum subspecies at the species level. Curr Microbiol 74:1137–1147. https://doi.org/10.1007/s00284-017-1296-9.

50. Bi D, Zhu Y, Gao Y, Li H, Zhu X, Wei R, Xie R, Wei Q, Qin H. 2021. A newly developed PCR-based method revealed distinct Fusobacterium nucleatum subspecies infection patterns in colorectal cancer. Microb Biotechnol 14:2176–2186. https://doi.org/10.1111/1751-7915.13900.

51. Karpathy SE, Qin X, Gioia J, Jiang H, Liu Y, Petrosino JF, Yerrapragada S, Fox GE, Haake SK, Weinstock GM, Highlander SK. 2007. Genome sequence of Fusobacterium nucleatum subspecies polymorphum - a genetically tractable fusobacterium. PLoS One 2:e659. https://doi.org/10.1371/journal.pone.0000659.

52. Boutaga K, van Winkelhoff AJ, Vandenbroucke-Grauls CM, Savelkoul PH. 2005. Periodontal pathogens: a quantitative comparison of anaerobic culture and real-time PCR. FEMS Immunol Med Microbiol 45:191–199. https://doi.org/10.1016/j.femsim.2005.03.011.

53. Oshima M, Oshima H, Kitagawa K, Kobayashi M, Itakura C, Taketo M. 1995. Loss of Apc heterozygosity and abnormal tissue building in nascent intestinal polyps in mice carrying a truncated Apc gene. Proc Natl Acad Sci U S A 92:4482–4486. https://doi.org/10.1073/pnas.92.10.4482.

54. DeStefano Shields CE, Van Meerbeke SW, Housseau F, Wang H, Huso DL, Casero RA, O'Hagan HM, Sears CL. 2016. Reduction of murine colon tumorigenesis driven by enterotoxigenic Bacteroides fragilis using cefoxitin treatment. J Infect Dis 214:122–129. https://doi.org/10.1093/infdis/jiw069.

55. Chen S, Zhou Y, Chen Y, Gu J. 2018. fastp: an ultra-fast all-in-one FASTQ pre-processor. Bioinformatics 34:i884–i890. https://doi.org/10.1093/bioinformatics/bty560.

56. Bankevich A, Nurk S, Antipov D, Gurevich AA, Dvorkin M, Kulikov AS, Lesin VM, Nikolenko SI, Pham S, Prjibelski AD, Pyshkin AV, Sirotkin AV, Vyahhi N, Tesler G, Alekseyev MA, Pevzner PA. 2012. SPAdes: a new genome assembly algorithm and its applications to single-cell sequencing. J Comput Biol 19:455–477. https://doi.org/10.1089/cmb.2012.0021.

57. Tanizawa Y, Fujisawa T, Nakamura Y. 2018. DFAST: a flexible prokaryotic genome annotation pipeline for faster genome publication. Bioinformatics 34:1037–1039. https://doi.org/10.1093/bioinformatics/btx713.

58. Seemann T. 2014. Prokka: rapid prokaryotic genome annotation. Bioinformatics 30:2068–2069. https://doi.org/10.1093/bioinformatics/btu153.

59. Ye Y, Doak TG. 2009. A parsimony approach to biological pathway reconstruction/inference for genomes and metagenomes. PLoS Comput Biol 5:e1000465. https://doi.org/10.1371/journal.pcbi.1000465.

60. Angiuoli SV, Dunning Hotopp JC, Salzberg SL, Tettelin H. 2011. Improving pan-genome annotation using whole genome multiple alignment. BMC Bioinformatics 12:272. https://doi.org/10.1186/1471-2105-12-272.

61. Price MN, Dehal PS, Arkin AP. 2009. FastTree: computing large minimum evolution trees with profiles instead of a distance matrix. Mol Biol Evol 26:1641–1650. https://doi.org/10.1093/molbev/msp077.

62. Edgar RC. 2010. Search and clustering orders of magnitude faster than BLAST. Bioinformatics 26:2460–2461. https://doi.org/10.1093/bioinformatics/btq461.

63. Strauss J, Kaplan GG, Beck PL, Rioux K, Panaccione R, Devinney R, Lynch T, Allen-Vercoe E. 2011. Invasive potential of gut mucosa-derived Fusobacterium nucleatum positively correlates with IBD status of the host. Inflamm Bowel Dis 17:1971–1978. https://doi.org/10.1002/ibd.21606.